A biological growth curve is a sum of two distinct S-curves

Shruti I S

Independent Researcher, Alappuzha, Kerala, India.

shruti.i.suresh@gmail.com

Abstract

A growing population consists of successive generations of individuals interacting with each other and the environment. At every instant, these individual interactions can lead to either promotion or restriction of the population growth. Thus, within a growing population, differences arise over time due to both extrinsic and intrinsic factors such as resource utilization, competition, age distribution etc. These differences can lead to divergence within the population growth. The sum of these differences is manifested as the net population growth. In this work, we propose that these differences that arise over time within a growing population can be represented as two distinct S-curves. The sum of these two S-curves results in the growth curve of a population. These differences also arise in the growth curves of mean individual attributes such as height or weight. We demonstrate this by applying the $a - m$ biological growth model on (i) the population growth curves of *Drosophila* and yeast and (ii) the growth curves of mean individual height of sunflower plants and the mean individual body weight of male white rats. Finally, we also discuss the results using a coordinate system with the two distinct S-curves as the axes.

1 Introduction

Based on his pioneering research on bacterial cultures, J. Monod described growth as a succession of phases characterized by variations in growth rate [1]. Although he has mentioned six phases, the order and presence of these phases can vary among different bacterial cultures. Since Monod's classification of growth phases is based on the growth rate we can generalize it to growth of all kinds. The phases are:

G1 lag phase (growth rate is null),

G2 acceleration phase (growth rate increases),

G3 exponential/linear phase (growth rate is constant),

G4 retardation phase (growth rate decreases),

G5 stationary phase (growth rate is null) and

G6 phase of decline (growth rate is negative).

In order to capture various phases, growth dynamics has been modeled as theory-based differential equations [2, 3, 4], empirical power laws [5] or polynomials [6, 7]. However, the phase of decline i.e. G6 has always been modeled separately [8].

Recently, a novel biological model (the $a - m$ model) was introduced that models growth using the continued fraction of linear growth [9]. The $a - m$ model is parameterized by two key factors: maximum growth rate m and a positive growth restricting term a. According to this model, the maximum growth rate is observed during the linear phase G3 when the non-linear restrictions of growth represented by a are minimal. This model was tested on population data of yeast cells and *Drosophila* as well as mean individual height and weight data of sunflower plants and male white rats respectively [9]. Taking the point of maximum growth rate as the origin, the $a-m$ model was fit to the data such that it effectively captured the acceleration (G2), linear (G3) and deceleration (G4) phases of growth that were in succession. The fit revealed that G2

and G4 phases are distributed symmetrically around G3 with respect to time. The $a-m$ model was also fit on individual human growth (height) data provided by R. Scammon [10, 11]. Although it did not fit well for the entire data, when portions of the data that showed S-shaped growth were selectively fitted, the $a-m$ model gave good results and even showed the same symmetry in G2 and G4 phases as mentioned before. Moreover, it was also observed that even for periods as long as 6 years this symmetry was maintained which means that the linear path of growth is restricted nonlinearly through a.

The $a-m$ model is obtained by introducing a parametric nonlinear term to the linear growth equation $\bar{N} = m\bar{t}$, given by

$$\begin{aligned} a\bar{N}^3 + \bar{N} &= m\bar{t} && (1)\\ \Rightarrow \bar{N} &= \frac{m\bar{t}}{1+a\bar{N}^2} \\ &= \frac{m\bar{t}}{1+a\frac{m^2\bar{t}^2}{\left(1+a\left(\frac{m\bar{t}}{1+\cdots}\right)^2\right)^2}} && (2)\\ &= -\frac{1}{3}\hat{y}^{\frac{1}{3}} + \frac{1}{a}\hat{y}^{-\frac{1}{3}} && (3) \end{aligned}$$

The last of the above equations is the analytical solution of the cubic equation (Eqn. (1)) with $\hat{y}$ given by

$$\hat{y} = -\left(\frac{27m\bar{t}}{2a}\right) + \sqrt{\left(\frac{27m\bar{t}}{2a}\right)^2 + \frac{27}{a^3}}. \tag{4}$$

In the above equations, $\bar{N} = N - N_m$, where N is the population size at time t, N_m is the population size at time t_m and $\bar{t} = t - t_m$. (N_m, t_m) is the point of linear growth at G3 phase which is also the point of maximum growth rate m. When $N = N_m$ and $t = t_m$, $\bar{N} = 0$ and $\bar{t} = 0$, respectively. Therefore, the point (t_m, N_m) can be considered as the origin of the model. The nonlinearity is introduced through the parameter a as a continued fraction.

The $a-m$ model is actually a sum of two parts (Eqn. (3)). They are:

$$S_1\colon\ -\frac{1}{3}\hat{y}^{\frac{1}{3}} \text{ and } S_2\colon\ \frac{1}{a}\hat{y}^{-\frac{1}{3}}. \tag{5}$$

Therefore, the actual population size is given by

$$N = S_1 + S_2 + N_m \ \text{ with the growth rate } \frac{dN}{dt} = \frac{m}{1+3a(S_1+S_2)^2}. \tag{6}$$

In the following section, a weighted sum of $a-m$ models is fit to the growth data of populations and individual attributes.

2 Weighted sum of $a-m$ models

In the previous section, the fitting of $a-m$ model on growth data is described where the origin is taken as the point of maximum growth. This way of fitting with a single origin was effective only for the part of the data that showed G2, G3 and G4 phases of growth. Therefore, instead of taking a single origin, multiple origins within the data points are selected. Each origin is selected following the procedure that was used to fit bacterial growth data in a previous work [12]. This means if two origins are selected, we get two different $a-m$ models and so on. The weighted sum of multiple $a-m$ models effectively captured all the phases of growth (G1 to G6). Thus the final model is a sum of $a-m$ models (Eqn. 6) of different origins with different growth rates. The single-origin $a-m$ model and the multi-origin models are compared in Table (1). Here, we have used the weighted sum N^{III} of three different $a-m$ models to fit the data [12]. This is because N^{III} showed good fits on the growth data considered in this work. It is given by

$$N^{III} = pN_1 + qN_2 + rN_3, \tag{7}$$

One-origin [9]	Multi-origin [12]
2- parametric	5- (or more) parametric
m is independent of a	m depends on a
m is directly estimated from the fitted curve	m is the peak value of the growth rate curve
Useful in fitting on G2,G3 and G4 phases	Useful in fitting all the phases G1 to G6
Captures either growth or decline	Captures growth and decline simultaneously
Helps to establish symmetric nature of G2 and G4	Helps to fit G1 to G6 as sums of S-curves

Table 1: Summary of models based on the continued fraction of straight lines.

where $N_1 = N(a, m_1, t_{m1}, N_{m1}), N_2 = N(a, m_2, t_{m2}, N_{m2})$ and $N_3 = N(a, m_3, t_{m3}, N_{m3})$. So, this model has 7 parameters. The above equation can be written in terms of S_1 and S_2 as

$$\begin{aligned} N^{III} &= p(S_1+S_2)_1 + pN_{m1} + q(S_1+S_2)_2 + qN_{m2} + r(S_1+S_2)_3 + rN_{m3} \\ \Rightarrow N^{III} &= \underbrace{pS_{11}+qS_{12}+rS_{13}}_{S_I} + \underbrace{pS_{21}+qS_{22}+rS_{23}}_{S_{II}} + \underbrace{pN_{m1}+qN_{m2}+rN_{m3}}_{\text{offset}}. \end{aligned} \tag{8}$$

Therefore we have,

$$N^{III} = S_I + S_{II} + \text{offset}. \tag{9}$$

Thus, the final model is expressed as a sum of two S-curves with an offset. This model is fit to the growth data shown in Figs. (1) to (4) using the `lmfit` package [13] with initial guesses: $p, q, r = 0$; $m_1, m_2, m_3 = 1$ and $a = 1e-3$ with $a > 1e-6$ for standardized data.

The growth rate of N^{III} is given by

$$\begin{aligned} \frac{dN^{III}}{dt} &= \frac{dS_I}{dt} + \frac{dS_{II}}{dt} \text{ or} \\ \frac{dN^{III}}{dt} &= \frac{pm_1}{1+3a(S_{11}+S_{21})^2} + \frac{qm_2}{1+3a(S_{12}+S_{22})^2} + \frac{rm_3}{1+3a(S_{13}+S_{23})^2}. \end{aligned} \tag{10}$$

Therefore, pm_1, qm_2 and rm_3 represent the maximum growth rate parameters of $a-m$ models of different origins. The implementation is as follows:

```
##Standardize data
xstd = (xdata - np.mean(x))/np.std(x)
ystd = (ydata - np.mean(y))/np.std(y)

##Define a-m model:
def N(x,a,m):
 haty = (-27*x*m/2/a+np.sqrt((27*x*m/a)**2+27/a**3))
 return haty**(-1./3)/a-haty**(1./3)/3
##Define the NIII model:
def NIII(x,a,m1,m2,m3,p,q,r):
 return p*(N(x-xc1,a,m1)+yc1) + q*(N(x-xc2,a,m2)+yc2) + r*(N(x-xc3,a,m3)+yc3)

##The origins (xc1,yc1),(xc2,yc2) and (xc3,yc3) are obtained using
##gradients among data points
grads=(ystd[1:]-ystd[:-1])/(xstd[1:]-xstd[:-1])
## Top 3 highest grads
mxpts = np.argpartition(np.abs(grads),-3)[-3:]
## Midpoints are obtained for i=0,1,2 using:
## (xstd[mxpts[i]]+xstd[mxpts[i]+1])/2
## (ystd[mxpts[i]]+ystd[mxpts[i]+1])/2
```

```
##Create model and its parameters with lmfit package
model = Model(NIII)
parms = model.make_params(a=dict(value=1e-3, min=1e-6),
            m1=dict(value=1), m2=dict(value=1), m3=dict(value=1),
            p=dict(value=0),q=dict(value=0),r=dict(value=0))
out = model.fit(ystd,parms,x=xstd)
yfit = out.best_fit

#Actual parameters from standardized data estimations
a,m1,m2,m3,p,q,r = out.values.values()
m1,m2,m3 = np.array([m1,m2,m3])*np.std(y)/np.std(x)
a = a/np.std(y)**2
```

The growth rates can be obtained directly as follows:

```
def Ngrad(x,a,m):
 return m/(1+3*a*N(x,a,m)**2)
NIIIgrad = p*Ngrad(x-xc1,a,m1) + q*Ngrad(x-xc2,a,m2) + r*Ngrad(x-xc3,a,m3)
```

We will now obtain values of parameters for various growth data below. For a linear model the maximum growth rate would be a weighted sum of the maximum growth rate parameters i.e. just the numerators in Eqn. (10). Therefore the linear growth rate is given as $m_{\text{linear}} = pm_1 + qm_2 + rm_3$. However, the actual growth rate m would be the maximum value of Eqn. (10). Thus, the discrepancies between m_{linear} and m indicates the effect of nonlinearity through a on the maximum growth rate.

2.1 *Drosophila* Population

We now consider the *Drosophila* population data provided by Pearl (Table 11 of [14]). In an earlier study [9], an $a - m$ model with origin ($t_m = 19.44, N_m = 166.56$) was fit on this growth data after excluding the first two data points. The maximum growth rate was found to be $m = 23.92$ for the selected data points.

In this work, we fit the N^{III} model on the growth data without omitting any of the data points as shown in Fig. (1a). The maximum growth rate parameters of $a-m$ models with origins '1', '2' and '3' (i.e., N_1, N_2 and N_3 of Eqn. (7)) are obtained as $pm_1 = -3.04$, $qm_2 = 17.04$ and $rm_3 = 13.48$, respectively.

Since pm_1 is negative, the corresponding $a-m$ model N_1 represents a decline in the number of individuals while N_2 and N_3 reflect the growth in number with time. The net maximum growth rate obtained from Fig. (1b) is $m = 24.75$. This maximum growth is less than the linear sum of N_1, N_2 and N_3 growth rates which is: $m_{\text{linear}} = pm_1 + qm_2 + rm_3 = 27.59$.

Role of a: As shown in Fig. (1), since both $q, r > 0$, the growth with rate $m_{\text{linear}} = 27.59$ is restricted positively to $m = 24.75$ through a. This disparity between m and m_{linear} indicates that a has a restricting effect on the linear growth which leads to the actual value of $m = 24.75$. This restriction occurs as a continued fraction (Eqn. (2)) which includes restrictions at all time scales.

In Fig. (1a), initially S_{II} is almost null while S_I grows. Therefore, S_I may represent the first generation of individuals while S_{II} represents the growth of subsequent generations. The offset given by Eqn. (8) is added to S_I for a better graphical representation. Here, the offset is added in such a way that the initial values of S_I lie along the N^{III} curve and the initial values of S_{II} are close to 0. In Fig. (1a), the growth of S_{II} accelerates when the growth of S_I starts to decline. This may be due to the disparities that arise within the population as younger individuals arrive. Thus the growth of a population is a combination of successive S-curves.

Fig. (1b) is given by Eqn. 10 which has no influence due to offset. From the figure, it is seen that the first generation S_I peaks before N^{III} does. While S_{II} peaks after N^{III}. This clearly indicates that growth occurs in successions. In the following section, we will extend this notion to the yeast population growth.

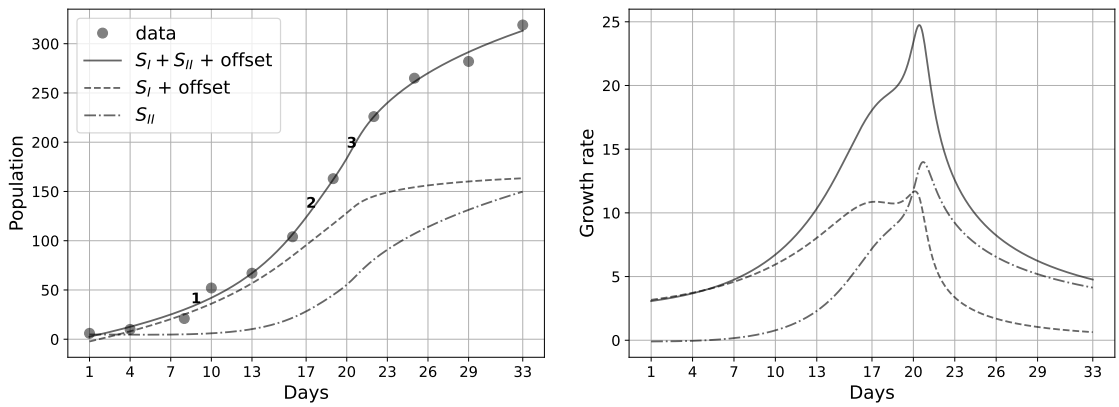

(a) $N^{III} = S_I + S_{II}+$ offset.

(b) Corresponding growth rates with a maximum peak value $m = 24.75$.

Figure 1: Successions in *Drosophila* growth data provided by Pearl [14].
$a = 1.83e-5,\ p = -0.38,\ q = 0.66,\ r = 0.11,\ m_1 = 8,\ m_2 = 25.82$ and $m_3 = 122.58$. Origins '1', '2' and '3' are also shown in (a).

2.2 Yeast Population

Using the yeast population data provided by Pearl (Table 9 of [14]), we use the N^{III} model to obtain a good fit and the resulting plots are shown in Fig. (2). The maximum growth rate parameters of N_1, N_2 and N_3 are given by $pm_1 = 170.33$, $qm_2 = 192.16$ and $rm_3 = -252.48$, respectively. Here, the negative value of rm_3 corresponding to the N_3 model indicates a decline in the number of yeast cells while N_1 and N_2 represent increase i.e. growth. The net maximum growth rate m is obtained from Fig. 2b as $m = 94.5$ which is again less than the linear sum $m_{\text{linear}} = pm_1 + qm_2 + rm_3 = 109.2$. As mentioned in the previous section, the disparity between m and m_{linear} is decided by the restricting effect that a has on linear growth.

Similar to the *Drosophila* plot, here too the S_I and S_{II} curves show opposing trends. The S_I curve increases initially while S_{II} remains stagnant. However, when S_I starts declining, S_{II} continues to show accelerated growth. From Fig. (2b), it is observed that S_I peaks before N^{III} and S_{II} peaks after N^{III},

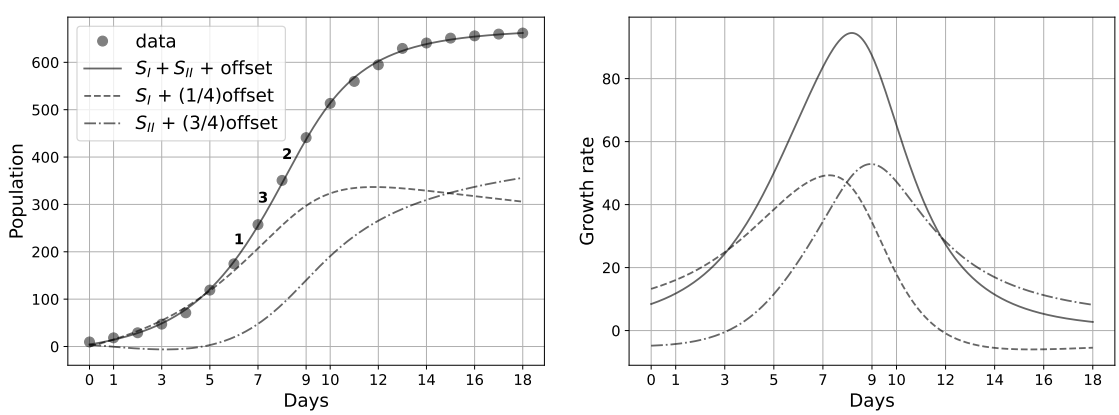

(a) $N^{III} = S_I + S_{II}+$ offset.

(b) Corresponding growth rates with a maximum peak value $m = 94.5$.

Figure 2: Successions in yeast growth data provided by Pearl [14].
$a = 8.36e-3, p = 138.48, q = 111.72, r = -277.45, m_1 = 1.23, m_2 = 1.72, m_3 = 0.91$.

thus indicating the shift in generations leading to the combined growth of the population. In the next two

sections, we apply the N^{III} model on mean individual attributes such as height and weight.

2.3 Height of *Helianthus* (sunflower) plants

The *Helianthus* growth data provided by Reed et al [15] consists of mean individual heights of fifty eight sunflower plants measured for eighty four days. Hence, here N represents the centimeter growth in height of *Helianthus* plants. Fig (3a) shows the fitting of N^{III} model on this growth data and the corresponding S_I and S_{II} curves. The maximum growth parameters of N_1, N_2 and N_3 are $pm_1 = 28.57$, $qm_2 = 15.33$ and $rm_3 = -36.3$, respectively. rm_3 being negative, we can conclude that N_3 represents decline while N_1 and N_2 represent growth in height.

From Fig (3b), the actual maximum growth rate is obtained i.e. $m = 5.32$. This is considerably lower than the linear maximum growth rate given by $mlinear = pm_1 + qm_2 + rm_3 = 7.54$. This indicates the highly nonlinear nature of this data as the restriction of linear growth through a is quite influential here. This is also reflected in the values of relative difference between m_{linear} and m given in Table (2). The *Helianthus* data shows the highest relative difference of 41.72% among all the data.

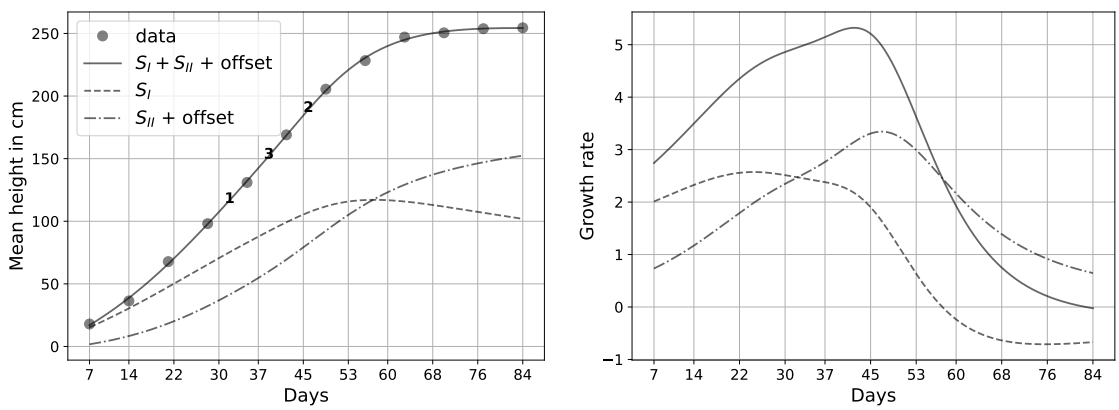

(a) $N^{III} = S_I + S_{II}+$ offset.

(b) Corresponding growth rates with a maximum peak value $m = 5.32$.

Figure 3: Successive growth in height of *Helianthus* plants based on the data provided by Reed et al [15]. $a = 7.22e-6, p = 4.77, q = 1.59, r = -6.6, m_1 = 5.99, m_2 = 9.64, m_3 = 5.5$

The S_I and S_{II} curves given in Fig. (3a) show highly opposing change in growth rates towards the end. This may be physically interpreted as older plants showing stagnation in growth thus reducing the mean height of the data.

2.4 Body weight of rats

The data considered here was provided by Donaldson [16]. Here N represents growth in body weight of male white rats measured in grams. As shown in Fig. (4a), the N^{III} model is fitted to the entire data and the maximum growth rate parameters are obtained as $pm_1 = -5.36$, $qm_2 = -0.24$ and $rm_3 = 8.01$. Here, both pm_1 and pm_2 corresponding to N_1 and N_2 are negative. Hence, N_1 and N_2 represent decline in body weight which means that a also plays a role in restricting decline. The value of maximum growth rate m is obtained from Fig. 4b as 2.47. This is more than the linear growth rate given by $pm_1 + qm_2 + rm_3 = 2.39$. This may be because the number of declining quantities that are being restricted is more than the growing quantity.

In Fig. (4a), it is seen that S_I first increases and then declines while S_{II} is almost null at first and then starts increasing gradually. The change in both the curves is so gradual that it almost appears linear. This is also reflected in the value of relative difference between m_{linear} and m given in Table (2) as 3.2%. This is the least among all the data indicating that nonlinear influence through a is minimal. This could be because there are more number of data points as the data was collected on a daily basis.

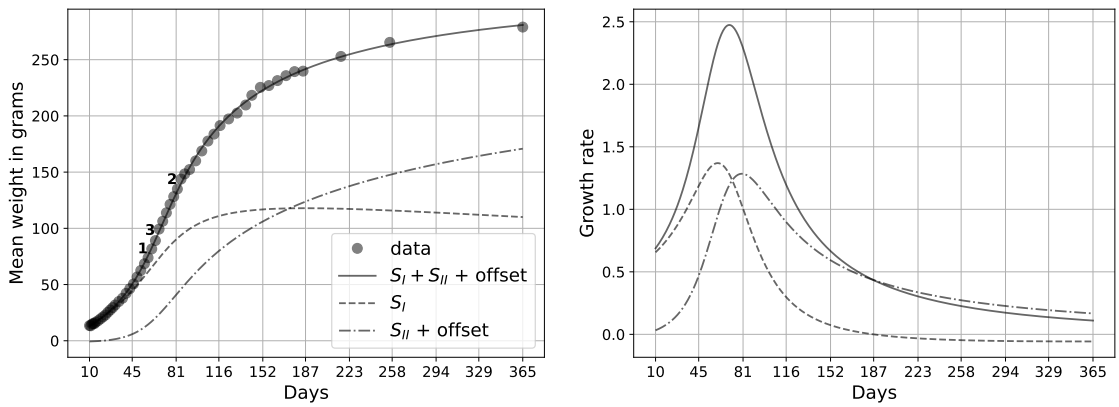

(a) $N^{III} = S_I + S_{II}+$ offset.

(b) Corresponding growth rates with a maximum peak value $m = 2.47$.

Figure 4: Successive growth in weight of male white rats based on the data provided by Donaldson [16]. $a = 9.08e-4, p = -17.74, q = -8.35, r = 21.65, m_1 = 0.302, m_2 = 0.029, m_3 = 0.37$

Growth data	$\frac{\lvert m_{\text{linear}} - m \rvert}{m} \times 100$
Drosophila	11.5%
Yeast	15.55%
Helianthus	41.72%
Male white rats	3.24%

Table 2: The nonlinearity through a is evaluated using the relative difference $|m_{\text{linear}} - m|/m$.

3 $S_I S_{II}$ plane

In this section, we present a coordinate system with the offsetted S_I and S_{II} as its axes. This is conceptually same as the $i, ii-$ plane given in [17]. Fig. (5) summarizes the growth curves presented in the previous section.

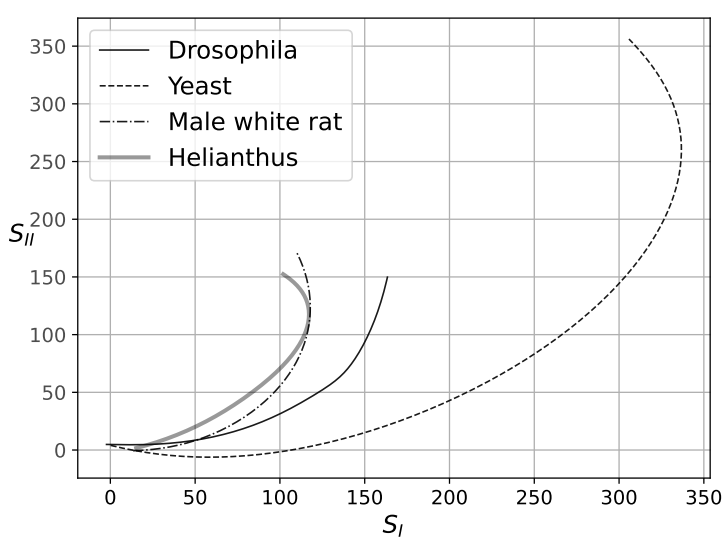

Figure 5: $S_I S_{II}$ plane including offsets from Figs. (1) to (4).

The offsets included in Fig. (5) are added in the same way as given in Figs. (1) to (4). In all the curves of Fig. (5), initially only S_I increases. Beyond a point, S_I either stagnates or starts to decline and S_{II} starts to grow. From Table 2, it is seen that the growth in mean height of *Helianthus* plants is highly nonlinear. This is also seen in Fig. (5). In the *Helianthus* growth curve, S_I shows a sudden decline while S_{II} starts to grow. The yeast data shows a similar trend as the *Helianthus* data but shows a more gradual decline of S_I. The rat data shows a gradual shift from S_I growth to S_{II} growth. The *Drosophila* growth data also shows a gradual shift yet not as smooth as the rat data.

The $S_I S_{II}$ coordinate system can be considered as a bounded $xy-$ plane [17]. This is because when $a = 0$ both S_I and S_{II} become unbounded and we get the original linear equation $\bar{N} = m\bar{t}$. This is same as the linear equation $y = mx$ on an $xy-$ plane with m as the slope. Conventionally, we use $y = mx$ and span the $xy-$ plane with a single parameter m. Having an additional parameter a causes the dependent variable y to increase at a slower rate than the independent x values by following the path of an S-curve. Thus, a can also be considered as a bounding parameter that transforms unbounded straight lines in to S-curves.

4 Conclusions

In this work, we have fitted the growth data of populations and individuals with a weighted sum of three $a - m$ models with different origins and with respective maximum growth or decline rate parameters. Thus, the weighted sum model includes both growth and decline and shows a good fit for all the data. This means that the net growth of populations and individuals is a combination of growth and decline. The net growth curve is also shown to be a sum of two offsetted S-curves. It is also observed that the growth rate curves derived from these two S-curves peak in successions and the curve of their sum i.e. the net growth rate peaks in between their peaks. The sum of the $a - m$ model's maximum growth rate parameters is considered as the linear growth and is compared with the actual maximum growth rate obtained as the peak value of the net growth rate curve. From this, the relative difference between linear growth rate and the actual growth rate is calculated which is helpful in analyzing the nonlinear dynamics of growth observed in these data. The growth data can be further visualized using a coordinate system with the offsetted S-curves as the axes. Since the growth data used here represents populations and individuals of different organisms, it can be concluded that biological growth is a combination of successive S-curves over time.

References

[1] Monod J. The growth of bacterial cultures. Annual Review of Microbiology. 1949; 3(1):371–94.

[2] Turner Jr, M. E., Bradley Jr, E. L., Kirk, K. A., and Pruitt, K. M. (1976). A theory of growth. Mathematical Biosciences, 29(3-4), 367-373.

[3] Baranyi, J., and Terry A. R. (1995). Mathematics of Predictive Food Microbiology. International Journal of Food Microbiology 26 (2): 199–218.

[4] Hall, Acar, B. G., and M. Barlow. (2013). Growth Rates Made Easy. Mol. Biol. Evol. 31: 232–38.

[5] Brown, J. H., Gupta, V. K., Li, B. L., Milne, B. T., Restrepo, C., and West, G. B. (2002). The fractal nature of nature: power laws, ecological complexity and biodiversity. Philosophical Transactions of the Royal Society of London. Series B: Biological Sciences, 357(1421), 619-626.

[6] Cross, J., Bradbury, R., Fulford, A. et al. Oral iron acutely elevates bacterial growth in human serum. Sci Rep 5, 16670 (2015). https://doi.org/10.1038/srep16670

[7] Wang, J., and Barger, K. (2024). ipolygrowth: an R package to calculate individual growth curve parameters from bacterial time series data. Microbiology Resource Announcements, 13(11), e00662-24.

[8] Bevilacqua, A., Speranza, B., Sinigaglia, M., and Corbo, M. R. (2015). A focus on the death kinetics in predictive microbiology: benefits and limits of the most important models and some tools dealing with their application in foods. Foods, 4(4), 565-580.

[9] Shruti, I. S., and Vijay Prakash, S. (2025). A biological growth model using continued fraction of straight lines, bioRxiv doi:10.1101/2025.01.07.631841.

[10] Scammon, R. E. (1927). The first seriatim study of human growth. American Journal of Physical Anthropology, 10, 329–336.

[11] Miller, E. M. The first Seriatum study of growth by R. E. Scammon (2018). American Journal of Physical Anthropology, 00:1–6.

[12] Shruti, I. S., and Vijay Prakash, S. (2025). Fitting multiple bacterial growth data using continued fraction of straight lines, bioRxiv doi:10.1101/2025.01.27.634991.

[13] Newville, M., Stensitzki, T., Allen, D. B., Rawlik, M., Ingargiola, A., and Nelson, A. (2016). LMFIT: Non-linear least-square minimization and curve-fitting for Python. Astrophysics Source Code Library, ascl-1606.

[14] Pearl, R. (1926). The biology of population growth. New York: Alfred A Knopf, Inc. Ch. 1-2.

[15] Reed, H. S., and Holland, R. H. (1919). The growth rate of an annual plant Helianthus. Proceedings of the National Academy of Sciences, 5(4), 135-144.

[16] Donaldson, H. H. (1906). A comparison of the white rat with man in respect to the growth of the entire body. Boas Anniversary Volume, New York.

[17] Vijay Prakash S. (2024). Real-valued continued fraction of straight lines. arXiv preprint arXiv:2412.16191.